Heliyon 10 (2024) e25376

Contents lists available at ScienceDirect

Heliyon

journal homepage: www.cell.com/heliyon

Research article

# Modeling and optimization of compaction pressure, **binder percentage** and retention time in the production process of carbonized sawdust-based biofuel briquettes using response surface methodology (RSM)

Junior Maimou Nganko [a,b,c,*], Ekoun Paul Magloire Koffi [a,**], Prosper Gbaha [a], Alpha Ousmane Toure [b], Moustapha Kane [c], Babacar Ndiaye [c], Mamadou Faye [d], Willy Magloire Nkounga [b], Claudine Tiogue Tekounegning [e], Echua Elisabeth Jasmine Bile [a], Kouassi Benjamin Yao [a]

[a] *Laboratory of Industrial Processes of Synthesis of the Environment and New Energy National Polytechnic Institute Felix Houphouët Boigny, BP:1093 Yamoussoukro RCI, Ivory Coast*
[b] *Laboratory of Water Energy Environment and Industrial Processes ESP-Cheikh Anta Diop University, BP:5085, Dakar-Fann, Senegal*
[c] *Center for Studies and Research on Renewable Energies, Cheikh Anta Diop University BP:476, Senegal*
[d] *The Institute of Applied Nuclear Technology, Cheikh Anta Diop University, BP:5085, Dakar-Fann, Senegal*
[e] *Biotechnology and Animal Productions, Aquaculture Advanced School of Agriculture, Forestry, Water and Environment the University of Ebolowa, PO Box 786, Ebolowa, Cameroon*

A R T I C L E I N F O

*Keywords:*
Sawdust
Biofuel briquettes
Response Surfaces Methodology (RSM)
Binder
Higher Heating Value (HHV)

A B S T R A C T

The importance of parameters such as compaction pressure, binder percentage and retention time and their interaction in the production of carbonized briquettes for domestic or industrial use cannot be overestimated, as they have a considerable impact on the properties of the resulting briquettes. This study used Box-Behnken Response Surface Methodology (RSM) and Analysis Of Variance (ANOVA) to show how the above parameters and their interactions significantly influence the Higher Heating Value (HHV), ash content and Impact Resistance Index (IRI) of the biofuels obtained. The briquettes are characterized in accordance with American Society for Testing and Materials ASTM D-(5865 and 3172). IRI is determined by the drop test. The Niton XLT900s X-ray fluorescence spectrometer is used for mineralogical analysis. The peel starch used as a binder is characterized by the Association of Official Agricultural Chemists standard. This starch has a starch purity of 89.8 %, an HHV of 13974 kJ/kg, a protein content of 4.79 % and a sugar content of 1.3 %. The HHV of the biofuels ranged from 23783 to 26050 kJ/kg, their ash content from 2.86 to 5.24 %, and the IRI from 136.36 to 500 %. The significant effect of binder on these results is confirmed ($p < 0.05$). The Standard deviations of $\pm$ 21.425 kJ/kg, $\pm$ 0.021 % and $\pm$ 2.121 % were obtained between the experimental values and those of the mathematical models developed to predict HHV, ash content and IRI. The optimum parameters for industrial biofuel production correspond to a binder percentage of 10 %, a compaction pressure of 75 kPa and a retention time of 7.49 min. The experimental results under these conditions are: 25596 kJ/kg,

* Corresponding author.Laboratory of Industrial Processes of Synthesis of the Environment and New Energy National Polytechnic Institute Felix Houphouët Boigny, BP:1093 Yamoussoukro RCI, Ivory Coast.
** Corresponding author.
*E-mail addresses:* junior.nganko21@inphb.ci (J.M. Nganko), ekoun.koffi@inphb.ci (E.P.M. Koffi).

https://doi.org/10.1016/j.heliyon.2024.e25376
Received 5 October 2023; Received in revised form 29 December 2023; Accepted 25 January 2024
Available online 1 February 2024

3.01 % and 375 % for HHV, ash content and IRI. In correlation with the absence of certain heavy metals, the study confirms that the briquettes produced are suitable for domestic use.

## 1. Introduction

These days, particular attention is paid to the development of renewable energies. Access to energy is now considered a fundamental right and a necessary condition for the development process [1,2]. However, it is estimated that around a third of the world's population still uses wood and coal as domestic fuel [3]. The same source indicates that the use of these wood fuels contributes significantly to deforestation. The need for accessible, renewable and environmentally-friendly energy is therefore felt. In addition, world leaders are promoting initiatives to produce, distribute and consume new energies at the expense of their so-called fossil fuel or polluting competitors (Chen et *al.*, 2020). In the face of these challenges, the energy potential and availability of biomass make it an excellent alternative (Kyaw et *al.*, 2020) because it makes a significant contribution to increasing energy diversity (Wu et *al.*, 2022). However, low energy density, size diversity, high moisture content are undesirable properties that hinder the use of certain biomasses as fuels [4]. These properties make them difficult to handle, store and transport. Certain techniques enable to considerably improve the properties of these fuels (Shen et *al.*, 2021). The technique most commonly used for this purpose is briquetting (Sunnu et *al.*, 2021; Wang et *al.*, 2020). However, briquetting alone does not meet all expectations [5] because briquette properties are influenced by a number of factors, such as the nature of the precursor material, and operating parameters. Several studies have reported that carbonizing biomass before compaction not only improves mechanical and physico-chemical properties, but also facilitates handling and storage and reduces moisture content (Wilczyński et *al.*, 2021; Wu et *al.*, 2022). This work focuses on the modeling and optimization of operating parameters such as compaction pressure, binder percentage and retention time in the process of converting carbonized sawdust into fuel briquettes. Several researchers have also demonstrated the importance of binders in the production of biofuels from carbonized or non-carbonized biomass, in this case (Husain et *al.*, 2002) who used palm fibers and shells with cassava starch as a binder (Teixeira et *al.*, 2010), have produced briquettes using bagasse and cassava starch as a binder (Bazargan et *al.*, 2014), have valorized palm kernel shells into biofuel with cassava starch as a binder (Sen et *al.*, 2016), have developed biofuels based on cassava rhizomes, with cassava starch and molasses as binders [6], have produced fuel briquettes from peanut shells and bagasse with cassava starch and wheat starch as binders (Aransiola et *al.*, 2019), have produced briquettes from carbonized corn cobs, with gelatin and cassava starch as binders (Narzary et *al.*, 2020), have proposed biofuels from dried leaves and rice husks with taro gel as a binder (Adu-Poku et *al.*, 2022), have proposed fuel briquettes made from rice husks and corn cobs, with cassava flour as a binder. However, with the evolution of research, cassava starch is now being used in many other sectors (Jayakumar et *al.*, 2023), have used it to produce second-generation bioethanol (Weligama et *al.*, 2023a), produced biodegradable food packaging from cassava starch, and (Fasheun et *al.*, 2023) have also produced hydrogen by dark fermentation from cassava starch. In addition to these numerous demands, biofuels will contribute around 17 % of growth in the use of cassava and its derivatives between now and 2028 [7]. This literature provides ample evidence of the need to find other sources of binders to replace cassava starch in the production of fuel briquettes. because its use to develop biodegradable food packaging, hydrogen and bioethanol will in future create conflicts of use and unnecessary competition between these sectors and the biofuels production field [8]. As a result, starch will become more solicited, expensive and scarce, and the cost price of fuel briquettes will rise. In addition to the problem of finding a new binder for biofuels and reducing the use of cassava and its derivatives as human foodstuffs, the literature consulted on biofuel production did not address the optimization of operating parameters such as compaction pressure, binder percentage and retention time. In addition, the reactors used in these studies did not allow the pyroligneous liquid to be recovered. Finally, none of these studies used Box-Behnken designs to investigate the influence of binder percentage, compaction pressure and retention time on biofuel characteristics such as higher heating value, ash content and impact resistance index. To overcome these shortcomings, this study adopts a three-stage approach. First, it focuses on the search for a new binder that can substitute cassava starch for biofuel production, in order to anticipate possible conflicts of use in the future. Secondly, to design a reactor for the thermochemical treatment of biomass to recover solid and liquid products. Finally, to model, optimize and study the influence of operating parameters (binder percentage, compaction pressure and retention time) on biofuel characteristics (higher heating value, ash content and impact resistance index), with the aim of producing quality briquettes in sufficient quantity.

Some researchers (Garrido et *al.*, 2017; [9]) have reported that sawdust is continuously open-burned, a common practice in many African wood-producing countries. The results of a survey conducted between February and April 2022 in the Republic of Ivory Coast among wood-processing units, professional organizations in the wood-processing sector and the forestry administration corroborate these researchers' findings. The aim of this survey was to ascertain the current availability and use of sawdust, in order to explore the possibilities for its valorization to reduce local residents' dependence on wood as a domestic fuel. Thus, the use of sawdust for the study proposes an alternative solution to open burning, offering a more responsible and sustainable management method.

The main objective of this study is to model, optimize and analyze the influence of operating parameters on the characteristic properties of biofuel briquettes produced from carbonized sawdust. The binder used and the briquettes obtained were characterized in accordance with [10] and ASTM D – (3172 and 5865) standards respectively. Based on the characterization results, the study assessed the possibility of replacing cassava starch, traditionally used in biofuel production, with potato peel starch.

The production of the briquettes with the optimum parameters determined showed high calorific value, high impact resistance index, low ash content and absence of certain heavy metals, confirming their suitability as a domestic fuel. In addition, the study identified the limitations of the proposed reactor for thermochemical processing, and made recommendations for future research.

Optimizing operating parameters is beneficial for producing briquettes on an industrial scale. Among the methods that can be used for this purpose, the Box-Behnken Response Surface Methodology (RSM) is recognized as one of the most effective (Ahmad et *al.*, 2017; Dam et *al.*, 2022). This statistical approach allows us to obtain maximum information with minimum experience (Mohammad et *al.*, 2014). It consists in modeling, optimizing and analyzing problems where several factors influence a response of interest. To this end, compaction pressure, binder percentage and retention time are modeled and optimized by the MSR, then their influence on the properties of the resulting briquettes is studied.

The innovations in this study include *(i)* recovery of potato peelings to produce a binder that can replace the cassava starch currently used to produce fuel briquettes. *(ii)* Development of mathematical models to determine higher heating value, ash content and impact resistance index with low costs. *(iii)* Determination and validation of the optimum parameters for producing fuel briquette at industrial-scale. *(iv)* A reactor to recover pyroligneous liquid during thermochemical treatment is designed.

## 2. Material and methods

### 2.1. Study zone

The biomass used is collected in the industrial zones of Ivory Coast (Abidjan, Adzopé and Yamoussoukro) shown on the map in Fig. 1.

### 2.2. Sampling and pretreatment of biomass

The raw material used is sawdust from Fraké (Terminalia superba Engl. & Diels), which is a tropical wood species with a density of 0.54. Following the survey previously conducted, it appears among the 5 most used species over the last 5 years (2017–2021). This biomass is obtained from the Abidjan-based wood processing company TRANCHIVOIRE. Since there are no standard sampling procedures specified for biomass materials (Parikh et *al.*, 2005), samples are carefully taken to ensure that they are distinct and unmixed.

Drying biomass on a rack in a direct dryer operating with solar radiation at 65 °C for 48 h in the dry season (November) reduced its moisture content (Fig. 2). The sorting process eliminates pieces of bark, scrap wood and metal. Before and after drying, the moisture content of the biomass is determined using a HUMID Check (made in British Serial N°: 11057183). Once pre-treatment is complete, the process moves on to carbonization.

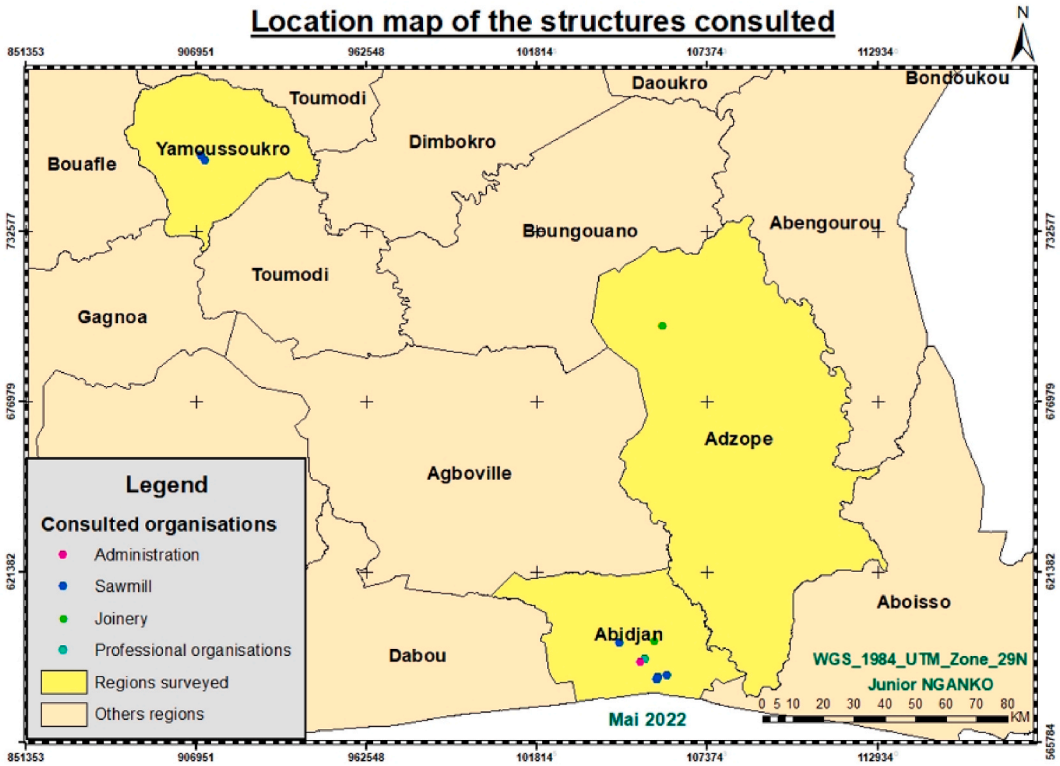


**Fig. 1.** Location map of the structures consulted during the survey and sampling.

**Fig. 2.** Biomass in the dryer.

### 2.3. Thermochemical treatment and pulverization of biomass

Thermochemical treatment is carried out in a retort furnace equipped with piping for the recovery of pyroligneous liquid. The process begins with the introduction of biomass into the furnace, followed by the installation of thermocouple probes to monitor temperatures. Once combustion has started, the vents are closed and the carbonization process is carefully monitored, ensuring that the various temperatures are recorded in the thermocouple's memory card. Three measurement points are taken into account: one inside the pyrolyzer (T1) and two outside (T2 and T3), as shown in Fig. 3a, which represents the reactor model, while Fig. 3b shows the actual image of the device. At the end of this stage, the carbonized product is unloaded and stored in a hermetically sealed container for 3 h to stop the carbonization process. Once cooled, the biochar is pulverized in a metal mortar to homogenize its granulometry, then sieved using a 1 mm mesh sieve (RETSCH, made in Germany, serial number: 5939814).

Table 1 shows the different parts of Fig. 3a.

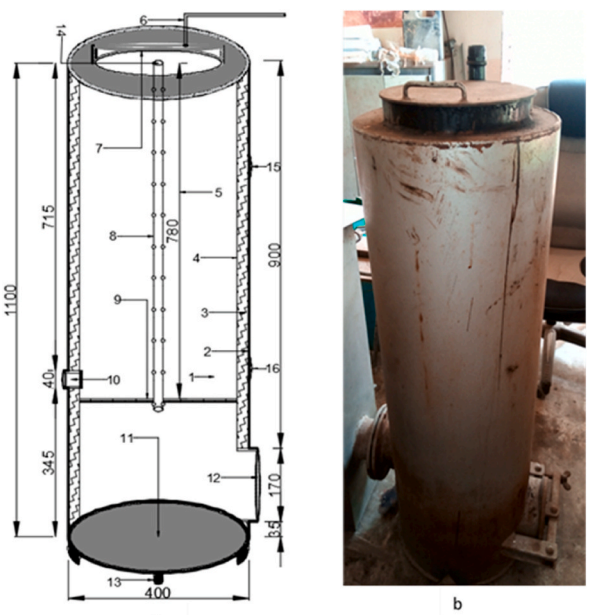


**Fig. 3.** Reactor used for carbonization: schematic view (a); real image(b).

**Table 1**
Coding of the reactor parts in Fig. 3 a.

| References | Significations |
|---|---|
| 1 | Carbonization dome |
| 2 | Exterior wall |
| 3 | Glass wool insulation |
| 4 | Interior wall |
| 5 | Useful height |
| 6 | Recovery port for pyroligneous liquid |
| 7 | Hermetic cover |
| 8 | Oxygenation column |
| 9 | Fine mesh for retention |
| 10 | Synthesis gas collection port |
| 11 | Reactor bottom |
| 12 | Biochar discharge unit |
| 13 | Reactor support |
| 14 | Temperature measuring point (T1) |
| 15 | Temperature measuring point (T2) |
| 16 | Temperature measuring point (T3) |

Once the thermochemical treatment is completed, the next step is the preparation of the binder and the formulation of the samples followed by the densification.

### *2.4. Binder preparation, characterization, formulation and mixing (binder & charred sawdust)*

#### *2.4.1. Starch isolation*

To produce the binder, potato peelings were collected from the university canteen, grated and rinsed with tap water to remove sand and other materials that could damage the mixer blades. They are then ground using a blender (Silver Crest), water is added and a 1 mm mesh sieve is used to separate the solution. The filtrate is left to settle for 24 h, and the starch milk recovered is oven-dried for 48 h at 40 °C.

#### *2.4.2. Characterization of the flour obtained*

The flour obtained is characterized according to the standardized method of the Association of Official Agricultural Chemists [10].

*2.4.2.1. Humidity levels.* It is determined by gravimetric heating (130 ± 2 °C for 2h) from a 2–3g sample.

*2.4.2.2. Ash content.* Ash content is determined in accordance with standard NF 03–720 (1981) at 900 ± 25 °C in a muffle furnace.

*2.4.2.3. Starch content.* The modified and standardized Ewers polarimetric method, ISO 10520 (1997) is used for starch determination. The polarimeter is a Bellingham Stanley ADP220 (Kent, England) with a specific rotation of 184° for pure starch. The following equation (1) is used to calculate the percentage of starch in flour:

$$\%\text{starch} = 9,4\left(\frac{S}{m_1} \times \frac{MS - S'}{m_2 \times MS}\right) \quad (1)$$

S: total rotatory power of the sample solution,
S': rotatory power of optically active substances soluble in 40 % ethanol,
$m_1$: mass of test sample used to determine S,
$m_2$: sample mass used to determine S′,
MS: dry matter content of the sample.

*2.4.2.4. Determination of soluble sugars.* Soluble sugars are extracted with alcohol and determined by the phenol-sulfuric acid colorimetric method [11]. Optical density at 490 nm was measured using a UV visible spectrophotometer UV-2401 PC Shimatzu (Kyoto, Japan) coupled to a computer (UV Probe software).

*2.4.2.5. Protein assay.* Protein levels in grain are determined using the Kjeldahl method (ISO 1871–1975), using a [12] Foss Tecator Technology (Hoganas, Sweden) and a Gerhardt vapodest 30 distillers (Bonn, Germany). A blank test and another using glycine (150 mg) are carried out. Protein content, based on 100g dry matter, is calculated using the following equation (2) and the conversion factor for feed.

$$\%\text{Protein} = \%N \times 6,25 \quad (2)$$

Where %N is the nitrogen rate calculated according to equation (3):

$$\%N = (V_1 - V_0) \times \frac{280}{P} \quad (3)$$

With:

$V_1$: volume of sulfuric acid solution used for titration, in ml,
$V_0$: volume of sulfuric acid solution used for blank titration, in ml,
P: mass of dry test sample, in g.

*2.4.2.6. Lipid determination.* Lipid concentrations are determined using the ISO3947 (1977) standard method. A Gerhard soxtherm (Bonn, Germany) is used. The mass of lipids is deduced from equation (4):

$$\%\text{lipid} = 100 \times \frac{m_2 - m_1}{P} \quad (4)$$

With:

$m_1$: mass of extraction flask, in g,
$m_2$: mass of extraction flask with extracted lipids, in g,
P: mass of dry test sample, in g.

*2.4.2.7. Carbohydrate content.* It is deduced from the moisture, protein, lipid and ash content using equation (5).

$$\%\text{carbohydrate} = 100 - (\%\text{moisture} + \%\text{protein} + \%\text{lipids} + \%\text{ash}) \quad (5)$$

### 2.4.3. Formulation and mixing

The char and starch flour are weighed using an electronic balance (CITIZEN SCALE made in USA serial Numbers N°:348660/13) with an accuracy of ±0.01 mg.

The solubilization of dry starch and water for the preparation of the binder is carried out at 1/10th of mass respectively [9]. The mixture is heated to 80 °C until the gel changes texture, thickens and becomes sticky (Agama-Acevedo et *al.*, 2011; Narzary et *al.*, 2020). During preparation, the mixture is stirred continuously with a spatula to prevent lumps from forming. The choice of potato peels for the binder is justified by their availability in Ivory Coast. The country consumes approximately 56782 t/year, broken down into 52 t/year grown locally and 56730 t/year imported [13]. Fig. 4 illustrates the process of binder preparation and mixing with carbonized sawdust. Fig. 4a shows the collected and washed peels, Fig. 4b illustrates the grinding device, while Fig. 4c shows the appearance of the binder after separation. In addition, Fig. 4d shows the textural appearance of the binder after drying, and finally, Fig. 4e shows the appearance of the mixture before compaction.

## 2.5. Densification and drying

The compression speed is approx. 1 cm/s and is operated by a crank handle. Briquette retention time under press varies from 4 to 8 min. Pressures range from 25 to 75 kPa. Fig. 5a shows the mechanical press used and Fig. 5 (a) shows the mechanical press used and Fig. 5 (b) illustrates the aspect of the briquettes obtained. After densification, the biofuels are left in the shade to stabilize for 24 h, to avoid thermal shocks that cause cracks in the walls. After stabilization, the products are dried in the sun for 21 days until substantially constant masses are obtained.

## 2.6. Industrial implementation scenario

For large-scale implementation, the scenario envisaged involves acquiring and fitting out a site dedicated to fuel briquette production, equipped with appropriate industrial machinery. The promoter then establishes sawdust recovery agreements with local sawmills. Similar agreements have been signed with university canteens and other major potato consumers.

Once the raw materials have been collected, the production of fuel briquettes begins on the specially designed site. The tooling

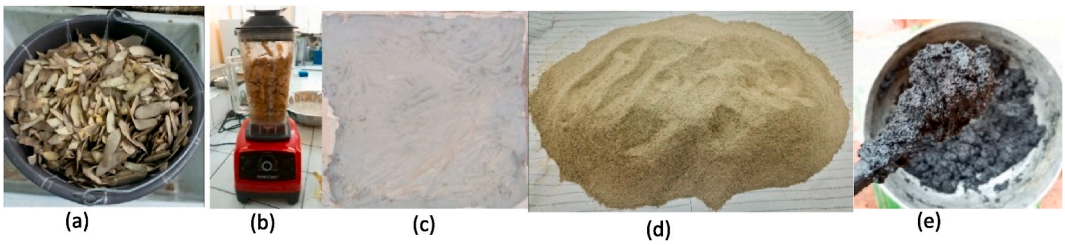


**Fig. 4.** Binder preparation and mixing: (a) peel collection and washing, (b) grinding, (c) drying, (d) dry starch, (e) appearance before compacting.

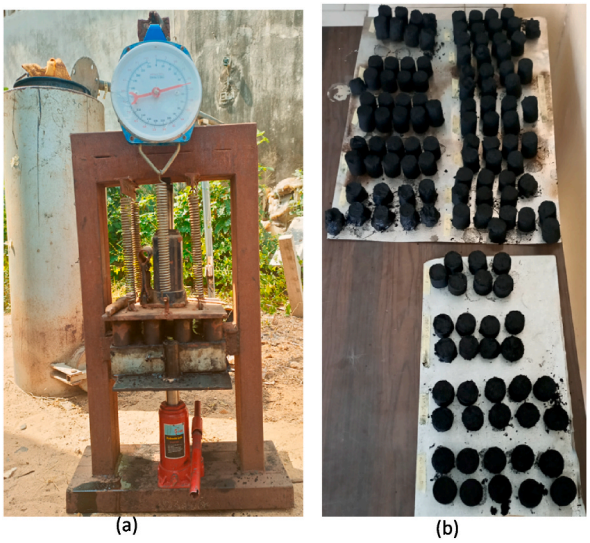


**Fig. 5.** Mechanical press used (a) aspect of the briquettes after compaction (b).

recommended for development is industrial equipment capable of processing large quantities of sawdust efficiently, while respecting the parameters and procedures established during the research and testing phase.

This industrial scenario makes it possible to set up a reliable and regular sawdust supply chain, while guaranteeing continuous and efficient production of combustible briquettes. This work is expected to be profitable, since it uses sawmill residues as raw material, thereby reducing the cost of supply. It offers the possibility of meeting the growing demand for biomass energy, while helping to reduce the use of fossil fuels or pollutants and promoting cleaner, sustainable energy. What's more, it enables residues to be recycled to reduce the pressure on tropical forests for energy purposes, and contributes to the development of local small-scale industry.

### 2.7. Characterization of composite biofuels

#### 2.7.1. Immediate or approximate analysis

Study analyses are carried out in accordance with the recommendations of the following standards (American Standard ASTM D-86, 2017). The same standards are used to characterize sawdust before carbonization and binder before solubilization. Samples are steamed in a BINDER oven, made in Germany, serial number 11–01662. The samples are then heated in a Nabertherm oven, made in Germany, serial number L3/11/B180. Each sample is analyzed three times, and the average is taken into account. The Elemental analysis of biofuels is determined in accordance with the Protocol defined by [14].

#### 2.7.2. Moisture content

The determination of sample moisture content is based on mass loss at 105 °C in the oven (Zinla et *al.*, 2021). Sample mass is measured as the sample dries to a stable mass. The difference between the initial and dried masses is used to determine the moisture content of the sample studied, according to equation (6).

$$H\% = \frac{M_2 - M_3}{M_2 - M_1} \times 100 \tag{6}$$

H: Moisture content (%);
$M_1$: Mass of the empty crucible (g);
$M_2$: Mass of crucible + sample (g);
$M_3$: Mass of crucible + sample, after heating (g).

#### 2.7.3. Volatile matter content

In practice, about 1g ± 0.05 mg of the briquette is crushed and placed in a closed crucible until a constant mass is obtained. The sample is then placed in a muffle furnace at a temperature of 950 °C ± 20 °C for 7min and weighed after cooling in a desiccator (Narzary et *al.*, 2020). Equation (7) is used.

$$VM = \frac{M_5 - M_6}{M_5 - M_4} \times 100 \tag{7}$$

VM: Volatile matter content (%)
$M_4$: Mass of empty crucible (g)

$M_5$: Mass of empty crucible + sample (g)
$M_6$: Mass of crucible + sample, after heating (g)

### 2.7.4. Ash content

The Ash represents the total mass of inorganic material remaining after complete combustion of the biofuel. For this purpose, about 1g ± 0.05 g of the solid fuel sample is heated in an oven for 2h at a reading temperature of 710 °C ± 5 °C (Narzary et *al.,* 2020). To obtain the ash mass, equation (8) is used.

$$\text{Ash} = \frac{M_9 - M_7}{M_8 - M_7} \times 100 \tag{8}$$

Ash: Ash content (%);
$M_7$: Mass of empty crucible (g);
$M_8$: Mass of empty crucible + sample (g);
$M_9$: Mass of crucible + sample after heating (g).

### 2.7.5. Fixed carbon content

The fixed carbon content is the proportion of carbon remaining after deduction of volatile compounds, moisture and ash. It is calculated as the difference between the total mass of the sample and the mass of water, volatile matter and ash (Zhuo et *al.*, 2021). Equation (9) is used.

$$\text{FC} : 100 - (\text{H\%} + \text{VM} + \text{Ash}) \tag{9}$$

FC: Fixed carbon content (%);
H: Moisture content (%);
VM: Volatile matter content (%);
Ash: ash content (%).

### 2.7.6. Mechanical properties of briquette biofuels

*2.7.6.1. Apparent density.* The density of briquettes is determined 30 days after they leave the press in accordance with [15]. An electronic laboratory balance with an accuracy of ±0.01 mg is used to determine the mass of the briquette biofuels. Its dimensions (heights and diameters) are measured with a caliper (HVC01200) to an accuracy of 0.05 mm. The density ρ (kg/m$^3$) is calculated by equation (10).

$$\rho = \frac{m}{\pi \times r^2 \times h} \tag{10}$$

m: Mass in (kg)
r: Radius of the briquette in (m)
h: Height of the briquette in (m)

*2.7.6.2. Impact resistance index (IRI).* The IRI represents the ability of briquettes to withstand various external forces during transport, handling and storage. According to (Bazargan et *al.*, 2014; Wu et *al.*, 2022), the Drop test was used to determine the IRI. The principle consists in repeatedly dropping the briquette (5 repetitions) from a height of 2 m onto a cement floor until it breaks up. According to [16] the minimum IRI value for domestic and industrial fuels is 50. The impact resistance index is determined using only parts weighing at least 5 % of the initial weight [17]. The IRI is calculated according to equation (11).

$$IRI = \frac{N}{n} \times 100 \tag{11}$$

IRI =Impact Resistance Index (%);
N: Number of drops;
n: Number of components that weighed at least 5 % of the initial weight of the briquette after N drops.

**Table 2**
Experimental area of the study.

| Factors | Units | Coded variables | Levels | |
|---|---|---|---|---|
| | | | Min | Max |
| Percentage of binder | % | $X_1$ | 10 | 20 |
| Compaction pressure | kPa | $X_2$ | 25 | 75 |
| Retention time | min | $X_3$ | 4 | 8 |

### 2.8. Statistical analysis

#### 2.8.1. Design of the experiment

The Box-Behnken designs used are Response Surface Methodologies (RSM) developed by George BOX and Donald BEHNKEN (Dam et *al.*, 2022). It is a statistical approach that provides maximum information on the variation of a parameter with minimum experimentation. The number of executions, N, to be performed is given by the relationship in equation (12):

$$N = 2k\ (k - 1) + r \tag{12}$$

k: Is the number of factors;

r: Is the number of replicates in the trials in the center of the experimental domain.

The various factorial combinations are given by a 3-factor Box-Behnken matrix with 3 levels, completely randomized and covering 17 experiments including 5 central points (Table 6). Design Expert 13.0.5.0 was used to model the system. The responses followed in this experimental design are higher heating value ($Y_1$), ash content ($Y_2$) and Impact Resistance Index ($Y_3$). The formula for calculating the response as a function of the factors is written as equation (13).

$$Y = b_0 + \sum_{i=1}^{n} b_i x_i + \sum_{i=1}^{n} b_{ii} x_i^2 + \sum_{i=1}^{n-1} \sum_{j=i+1}^{n} b_{ij} x_i x_j \tag{13}$$

Y represents the predicted response;

$b_0$: the constant coefficient;

$b_i$: the linear coefficients;

$b_{ij}$: the interaction coefficients;

$b_{ii}$; the quadratic coefficients;

$x_i$, and $x_j$ are the coded values of the operating parameters.

#### 2.8.2. Choice of the experimental field

The operating parameters studied during biofuel production are: binder concentration ($X_1$), compaction pressure ($X_2$) and retention time ($X_3$). The experimental range is shown in Table 2.

The choice of variation ranges for these parameters was guided by the work of [18,19] for compaction pressure and retention time respectively. Concerning binder percentage, below 10 %, the resulting briquettes disintegrated during ejection at the press die and their impact resistance index was undesirable. Above 20 %, the briquettes produced become more resistant. However, the drying time is longer and the higher heating value is considerably reduced. In addition, it is interesting to use a small amount of binder for briquette production as this is economical [20].

### 2.9. Mineralogical analysis by X-ray fluorescence

Mineralogical analysis is carried out according to (ASTM D4294, 2019) This analysis was used to determine the elemental mineralogical composition of the optimum sample using a "Niton XLT900s'' X-ray fluorescence spectrometer.

### 2.10. Calorific properties

The calorific value of a fuel represents the total amount of heat released by the complete combustion of 1 kg of that fuel [21]. It is expressed in (kJ/kg). There is the Higher Heating Value (HHV) and the Lower Heating Value (LHV). The water formed during combustion is released in liquid form in the first case, and in gaseous form in the second (Álvarez et *al.*, 2015). HHV is measured here using an automatic bomb calorimeter (PARR INSTRUMENT COMPANY made in USA N°:101A C20 032614 M4013) as recommended by (EN ISO 21654, 2021).

### 2.11. Energy density

Energy density represents the amount of energy contained in a given mass of a substance or product. Energy density is calculated according to equation (14)

$$E\,D = d.\ HHV \tag{14}$$

ED: Energy density ($kJ/m^3$);

HHV: higher heating value (kJ/kg)

d: apparent density of the briquette ($kg/m^3$);

The diagram in Fig. 6 summarizes the methodology used.

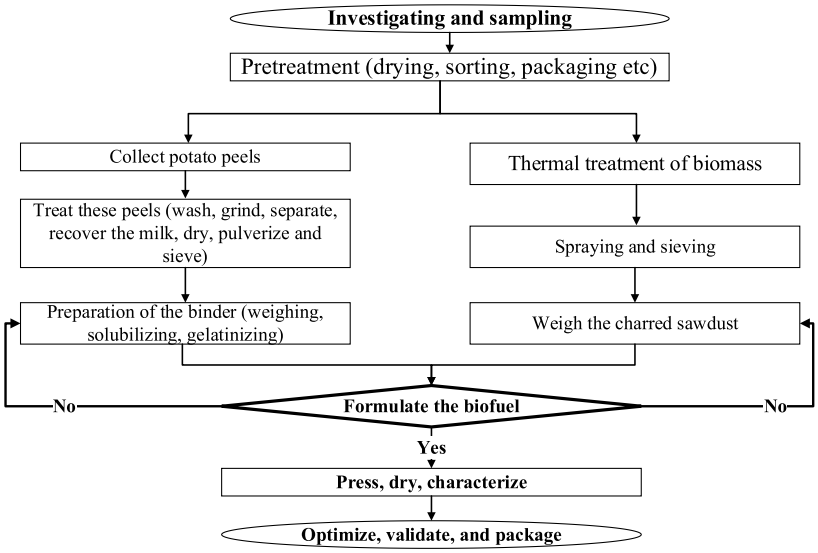


**Fig. 6.** Methodological synthesis.

## 3. Results and discussion

### 3.1. Survey and sampling

According to the data collected during the survey, the average volume of Fraké wood used over the last five years (2017–2021) is around 10 871 669 $m^3$/year, [22]. In addition, it was found that the material yield in wood processing units is low. Only around 45 % of the total roundwood volume is used as lumber. The remaining residues, such as slabs, edgings, sapwood (approx. 24 %), sawdust (approx. 16 %), heart defects (approx. 10 %), as well as off-cuts and trimmings (approx. 5 %). Among these residues, sawdust represents a significant and unused quantity. On average, around 1 739 467.04 $m^3$/year of Fraké sawdust has been generated over the past five years.

### 3.2. Carbonization

At the end of carbonization, the average time was 7h 25min, the mass yield 36.85 % and the pyroligneous liquid 69.78 ml. This yield is slightly higher than the 34 % obtained by (Temmerman et *al.*, 2019). This improvement may be due to the glass wool used to insulate the reactor walls.

The resulting "char" is shown in Fig. 7 (a) and the pyroligneous liquid in Fig. 7 (b).

The temperature vs. time profile obtained during carbonization is shown in Fig. 8.

The curves in Fig. 8 show the temperature profile as a function of time during the process. The T1 curve (temperature inside the reactor measured at point 14 in Fig. 3a) is well above T2 (temperature at point 15 in Fig. 3a) and T3 (temperature at point 16 in Fig. 3a) throughout the process. The wool used for insulation would be responsible for this heat retention inside the reactor. Since firing is upwards, for the first 120th minutes, (T2) and (T3) show the same rate. Then, when carbonization reaches full speed, (T2) increases

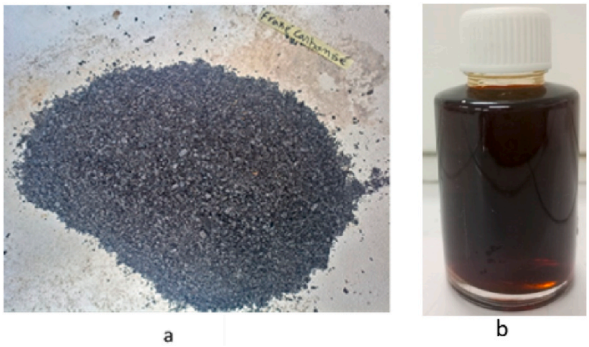


**Fig. 7.** Charred sawdust (a) pyroligneous liquid (b).

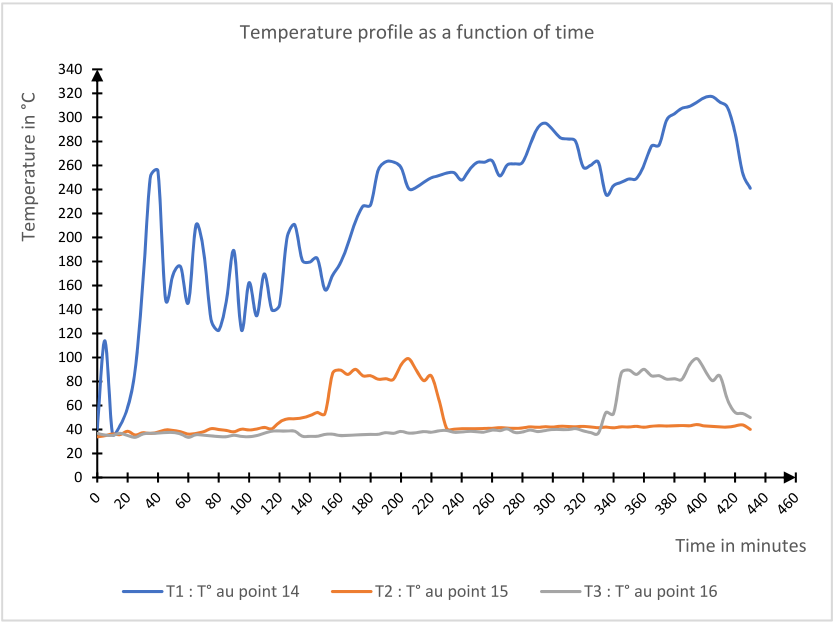


**Fig. 8.** Temperature profiles: (T1) temperature inside the reactor point 14 Fig. 3a, (T2) outside high point 15 Fig. 3a and (T3) outside low point 16 Fig. 3a.

from the 120th minute to the 230th minute, when it becomes stable again like (T3). Finally, when the fire reaches the bottom of the reactor at 335th minutes, (T3) increases until 430th minutes before dropping to the end of the process.

### *3.3. Binder preparation, formulation and mixing*

The mass yield between the starting peel mass and the finished product (dry powdered starch) is 22.48 %. The binder used in this study has not yet been used in the literature consulted. Table 3 shows the different materials, binders, their concentration, compaction pressure and densities of some biochar samples from the literature.

**Table 3**
Raw material, binder, binder concentration, compaction pressure and density of various briquettes.

| References | Raw materials | Binders | Binder concentration (%) | Compaction Pressure (MPa) | Density (g/cm$^3$) |
|---|---|---|---|---|---|
| [6] | Groundnut shells and bagasse | Cassava starch & wheat starch | 2.91–8.25 | <7 | 0.2–1.0 |
| (Husain et *al.*, 2002) | Palm fiber and shell | Cassava starch | 10 | 5–13.5 | 1.1–1.2 |
| (Sen et *al.*, 2016) | Rhizome of cassava waste | Molasses, starch and concentrated sludge | 30–40 | [a]n. a | 0.69–0.91 |
| (Teixeira et *al.*, 2010). | Sugar cane bagasse | Cassava starch | 8 | 6.43 | 1.12 |
| (Bazargan et *al.*, 2014) | Palm kernel shell | Cassava starch | 10 | 20–100 | 0.288–0.747 |
| (Adu-Poku et *al.*, 2022) | Rice husk, corn cobs, sawdust | Cassava flour | 10–20 | 10–30 | 0.444–0.498 |
| [23] | Rice husk, sawdust, bagasse | Glycerin | 0–30 | 10 | [a]n.d |
| (Narzary et *al.*, 2020). | Dry leaves, straw and rice husks, | Taro gel | 40 | [a]n.a | 0.233–0.234 |
| (Kivumbi et *al.*, 2021) | Fine charcoal | African elemi resin | 25–40 | 5.92–7.96 | 0.770–1.036 |
| (Aransiola et *al.*, 2019) | Charred Corn Raffle | Corn starch and gelatin | 10–30 | 0.05–0.15 | 0.729–0.987 |
| This research | Sawdust of wood Fraké | Starch from potato peels | 10–20 | 0.025–0.075 | 0.318–0.458 |

[a] n.a.: not available.

### 3.4. Densification and drying

The density of the samples varied from 318.31 to 458.12 kg/m$^3$. This value is lower than the 729–987 kg/m$^3$ of (Aransiola et *al.*, 2019) because they worked with a compaction pressure ranging from 50 to 150 kPa.

### 3.5. Immediate analysis and calorific properties

The results of the characterization tests and the higher heating values of the raw materials, binders and briquettes are shown in Table 4 and Fig. 9 respectively. Table 5 shows the properties of the binder discovered and used in this study.

On the sample coding, the letter (F=Fraké) represents the initial parent biomass, the first number the binder percentage, the second the compaction pressure and the last the retention time.

The results in Fig. 9 show the lowest ash content of 2.86 %, corresponding to sample $F_{10\text{-}50\text{-}8}$ with a binder concentration of 10 %, a compaction pressure of 50 kPa and a retention time of 8min. This value is lower than the 3.2 % obtained by (Sunnu et *al.*, 2021) because the parental biomass is not mixed with bark. The highest level of 5.24 % corresponds to sample $F_{20\text{-}25\text{-}4}$ with a binder/'char' ratio = 0.25, which is lower than the 6.5 % obtained by (Augou et *al.*, 2020) with a binder/sawdust ratio = 1. The highest moisture content of 6.18 % is in agreement with (Pallavi et *al.*, 2013) who attest that briquettes ignite rapidly when burned with low moisture content, without the appearance of slag.

The higher heating values (HHV) range from 23783 to 26050 kJ/kg, corresponding to samples $F_{20\text{-}50\text{-}4}$ and $F_{10\text{-}50\text{-}4}$ respectively. Tables 4 and 5 show the higher heating values for parent biomass (19565 kJ/kg) and binder (13974 kJ/kg) respectively. The evolution of the curve (Fig. 9) shows that an increase in the percentage of binder leads to a reduction in the higher heating value. However, for all samples, the higher heating value obtained respects the reference value of (Austrian standard M7135, 2021) (heating value $\geq$ 18000 kJ/kg). The highest HHV value of 26050 kJ/kg is lower than the 29700 kJ/kg obtained by (Kivumbi et *al.*, 2021), as they used charcoal fines as parent biomass and African elemi resin (*Canarium Schweinfurthii*) as binder.

The Elemental analysis of the biofuels reveals that among the samples, $F_{10\text{-}50\text{-}4}$ has the highest carbon content, at 65.35 %, while $F_{20\text{-}25\text{-}6}$ has the lowest, at 59.28 %. Hydrogen levels range from 4.54 % to 5.96 % for samples $F_{15\text{-}25\text{-}8}$ and $F_{15\text{-}50\text{-}6(1)}$ respectively. These values fall within the range recommended by [24], which recommends a range of 45 %–88 % for carbon and 4 %–6.5 % for hydrogen. Oxygen content varies between 23.9 % and 29.69 %, respectively for samples $F_{15\text{-}25\text{-}8}$ and $F_{20\text{-}50\text{-}4}$. As for sulfur, it was not detected in the samples, which corroborates the results from (Kivumbi et *al.*, 2021).

Table 5 shows the characteristics of the binder used. The starch purity of 89.8 % is satisfactory, as it is close to the 91.9 % obtained by [11]. A protein content of 4.79 is lower than the 6.9 % obtained by (Agama-Acevedo et *al.*, 2011). The type of raw material used and the testing protocols are thought to account for this difference. An acceptable HHV of 13974 kJ/kg means that the flour obtained can be used as a binder. The availability, accessibility and properties of potato peel starch, which improve the structural integrity and combustion characteristics of briquettes, favored its choice. What's more, the valorization of this agricultural waste can have a positive impact on local economies by creating opportunities for small businesses.

### 3.6. Mechanical properties and energy densities of developed biofuels

Fig. 10 shows the values for the mechanical and energy properties of the samples.

Density values range from 318.32 to 458.13 kg/m$^3$, corresponding to samples $F_{20\text{-}25\text{-}6}$ and $F_{10\text{-}75\text{-}6}$ respectively. The minimum value is higher than the 233 kg/m$^3$ obtained (Narzary et *al.*, 2020). This is justified by a mixture of sawdust and grass leaves at 50 % of each biomass in their study. The maximum value is less than 498 kg/m$^3$ obtained by (Adu-Poku et *al.*, 2022). The compaction pressure of up to 30 MPa used in their study may explain this difference. The energy density of a fuel represents the amount of energy stored per unit volume or mass. The energy density variation curve (Fig. 10) shows that it oscillates between 7560.38 and 11826.51 MJ/kg, corresponding to samples $F_{15\text{-}25\text{-}8}$ and $F_{10\text{-}75\text{-}6}$ respectively. This variation is associated with fuel density. Previous researchers [4] have reported that denser fuels have higher energy densities. The results of this study confirm those researchers' findings, as samples $F_{15\text{-}25\text{-}8}$ and $F_{10\text{-}75\text{-}6}$, with densities of 318.32 and 458.13 kg/m$^3$ respectively, have energy densities of 7560.38 and 11 826.51 MJ/kg each, respectively.

The impact resistance index of the samples varies between 136.36 and 500 % corresponding to samples $F_{10\text{-}25\text{-}6}$ and $F_{20\text{-}50\text{-}8}$ respectively. The minimum IRI of 136.36 % is 2.73 times higher than the 50 % threshold defined by (Bazargan et *al.*, 2014; [16]). This value confirms that the binder discovered by the study is suitable for fuel briquettes. Moreover, the maximum value of 500 % obtained at pressures of 75 kPa is the same as that obtained by (Adu-Poku et *al.*, 2022) at 30 MPa pressure and 20 % binder concentration. Fig. 11a and b shows, respectively, the appearance of samples lying and standing after five drops from a height of 2 m above the ground.

**Table 4**
Immediate analysis data of the parental biomass.

| Immediate analysis | | | | | Higher heating value (kJ/kg) |
|---|---|---|---|---|---|
| Samples | Humidity (%) | Volatile matter (%) | Ash (%) | Fixed carbon (%) | |
| Fraké | 09.04 | 82.75 | 0.63 | 7.58 | 19 565 |

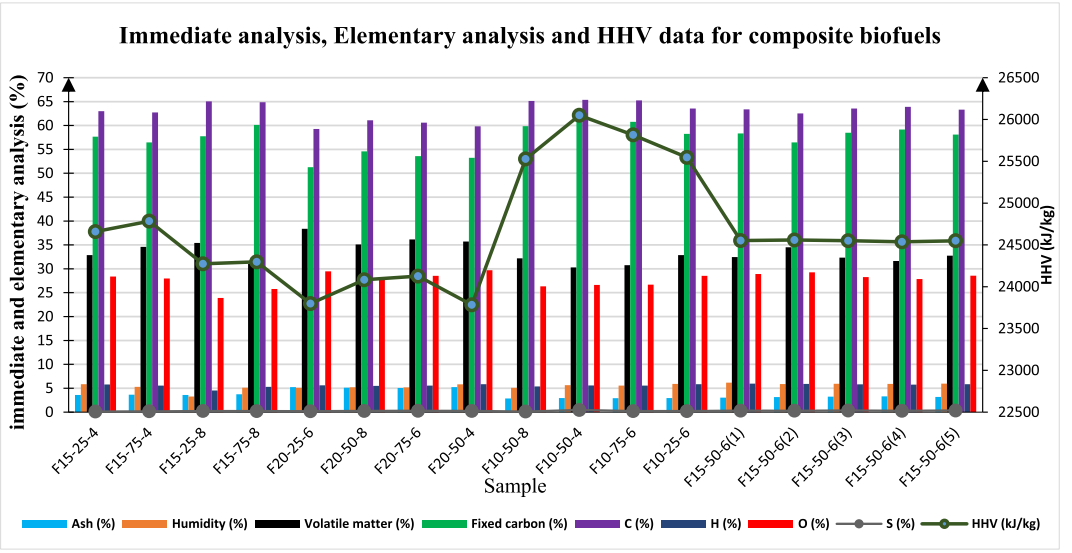


**Fig. 9.** The Immediate, Elemental and HCV analysis results for composite biofuels.
C: carbon; H: hydrogen, O: oxygen; S: sulfur; HHV: Higher Heating Value.

**Table 5**
Characteristic properties of the binder used.

| Properties | Results | Methods |
|---|---|---|
| Proteins (%) | 4.79 ± 0.045 | (NFV 18–100) |
| Humidity (%) | 10.30 ± 2.15 | ASTM D – (3172) |
| Ash content (%) | 1.91 ± 1.02 | ASTM D – (3172) |
| Lipids (%) | 0.15 ± 0.01 | NFV (03–905) |
| Carbohydrates (%) | 86.40 ± 2.04 | LUFF Schoorf |
| Sugars (%) | 1.30 ± 0.02 | LUFF Schoorf |
| Starch purity (%) | 89.8 ± 1.06 | ISO 10520 |
| Fixed carbon (%) | 9.08 ± 5.9 | ASTM D – (3172) |
| Volatile matter (%) | 78.71 ± 6.45 | ASTM D – (3172) |
| Higher heating value (kJ/kg) | 13 974 ± 105 | ASTM D – (5865) |

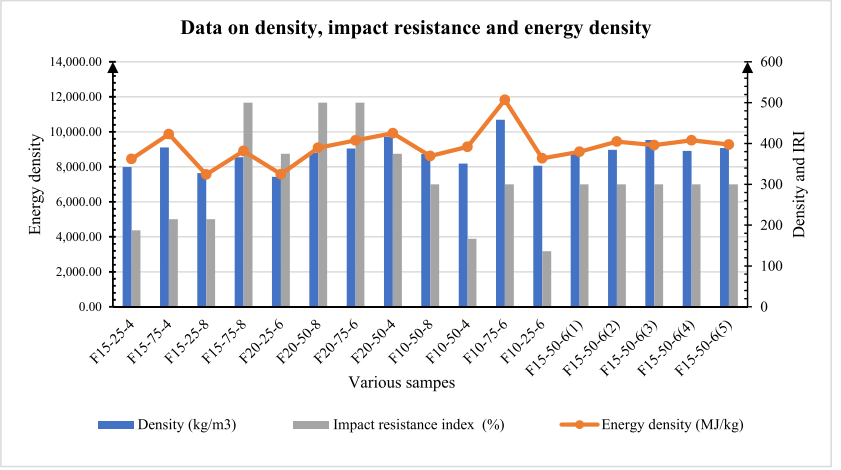


**Fig. 10.** Density, energy density and impact resistance index data for samples.

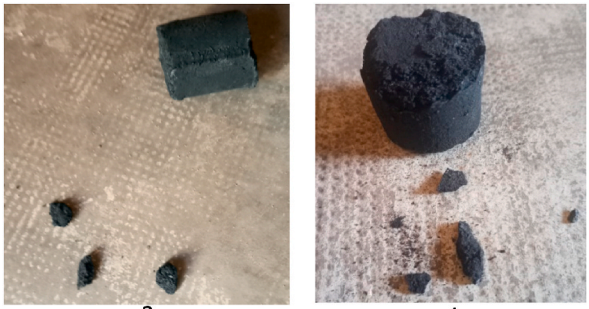


**Fig. 11.** Aspect of the samples lying (11a) and standing (11b) after 5 drops at 2 m from the ground.

### 3.7. Statistical analysis of the experimental results

#### 3.7.1. Development of the equations of the regression model

Analysis of the different models (linear, 2FI, quadratic and cubic) shows that the quadratic model is the most suitable for predicting responses, with the best correlation coefficients. The quadratic models combining responses to the study factors are given by equations (15)–(17).

- **Higher heating value**

$$Y1\ (kJ/kg) = +30\,587.375 - 643.390X_1 + 35.263X_2 - 303.4125X_3 - 3.078X_1X_2 + 58.075X_1X_3 + 2.99\,X_2X_3 + 10.588X_1^2 + 0.17\,192X_2^2 - 2.1375X_3^2 \quad (15)$$

- **Ash content**

$$Y2(\%) = -2.26125 + 0.57115X_1 + 0.00267X_2 + 0.13475X^3 + 0.00016X_1X_2 - 0.00525\,X_1X_3 + 0.00105X_2X_3 - 0.00848X_1^2 - 0.000107X_2^2 - 0.008625X_3 \quad (16)$$

- **Impact resistance index**

$$Y3\ (\%) = +237.625 - 20.525X_1 - 2.075X_2 - 25.25X_3 + 0.022X_1X_2 - 0.2X_1X_3 + 1.3X_2X_3 + 1.435X_1^2 - 0.033X_2^2 - 0.09375X_3^2 \quad (17)$$

#### 3.7.2. Statistical analysis of the models

Analysis of variance (ANOVA) is used to assess the relevance and significance of the models. The ANOVA results are summarized in Table 6. In accordance with (Bouazizi et *al.*, 2016 for p-values of less than 5 % ($P<0.05$) the models are significant.

Analysis of Table 6 shows that the main effect of binder percentage ($X_1$) significantly influences all responses. The effect of $X_1X_2$ and $X_1X_3$ interactions is significant on HHV, as they allow maximum drainage of the water used for binder solubilization. The impact resistance index, on the other hand, is influenced by the main effects $X_1$, $X_2$ and $X_3$. The interaction effect $X_2X_3$ is the only one that significantly influences the IRI.

#### 3.7.3. Analysis of responses

*3.7.3.1. Higher heating value.* Fig. 12a, b and c show the $X_1X_2$, $X_1X_3$ and $X_2X_3$ interactions respectively, and 12d the main effects of parameters on HHV.

Table 6 shows that the higher heating value is significantly influenced ($p < 0.05$) by all three factors as well as the $X_1X_2$ and $X_1X_3$ interactions with $R^2 = 97.12$ %, justifying the high consistency of the results. The curve in Fig. 12a shows that a minimum binder percentage (10 %) and a maximum compaction pressure (75kpa) result in a high HHV (approx. 27000 kJ/kg). This finding corroborates the work of (Sunnu et *al.*, 2021). Fig. 12b highlights the favourable conditions between binder percentage and retention time. A high HHV is obtained (approx. 26200 kJ/kg) with a low binder percentage (10 %) and a relatively short retention time (4min). Similar results are obtained by [4]. Fig. 12c has a non-significant effect ($p>0.05$) on HHV. Nevertheless, it stipulates that the best conditions under which to have a max HHV (around 25100 kJ/kg) are suitable for working with a pressure of 75kPa, and a retention time of 4min. A similar observation was made by (Yank et *al.*, 2016), reinforcing the reliability of the conclusions drawn by this study. Fig. 12d clearly show the main effects of parameters on HHV. They show that an increase in binder percentage and retention time leads to a decrease in HHV. On the other hand, increasing compaction pressure results in greater drainage of the water used for binder solubilization, leading to maximum HHV.

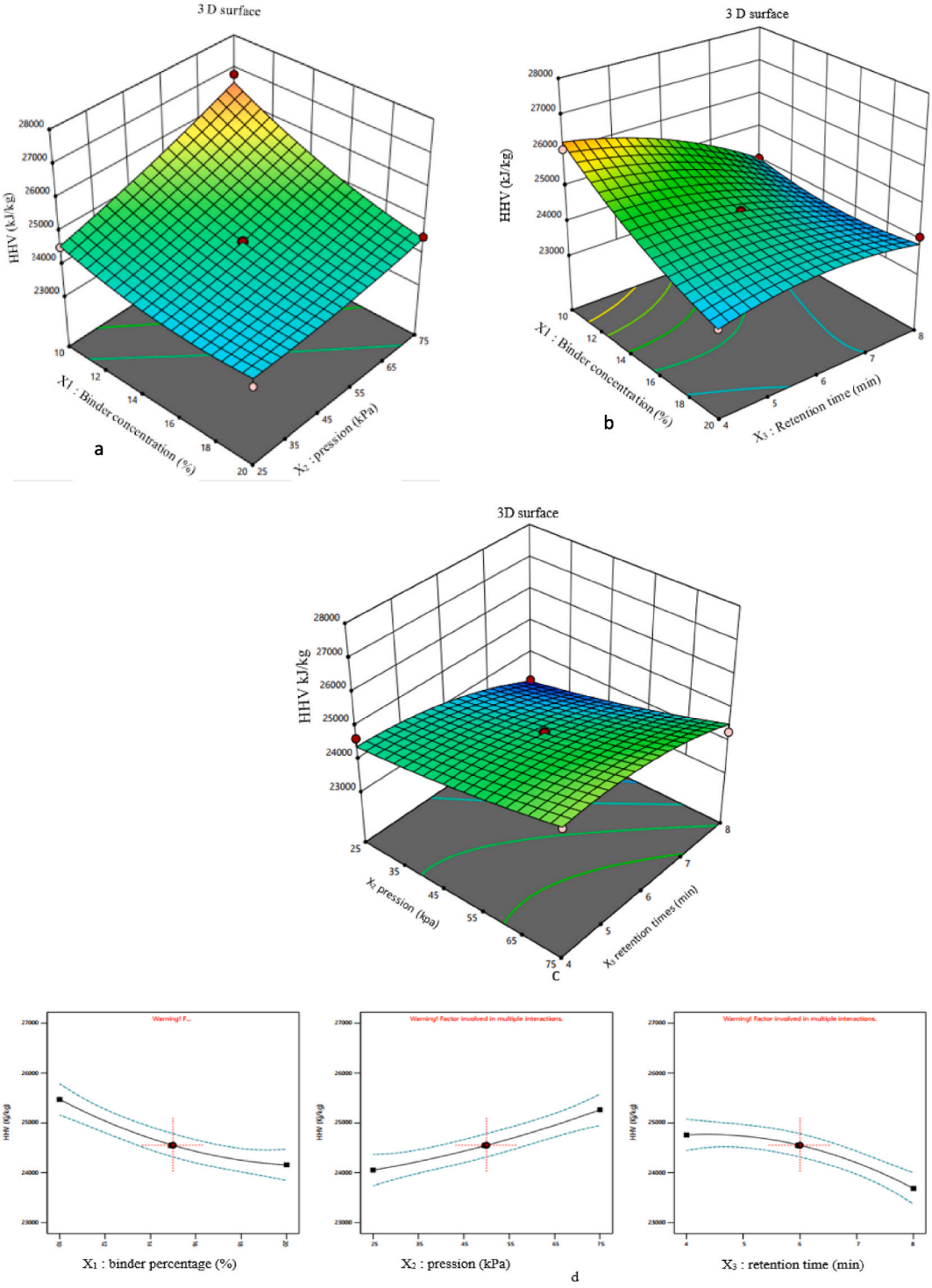


**Fig. 12.** Diagrams of response surfaces (a:$X_1X_2$), (b:$X_1X_3$) and (c:$X_2X_3$) respectively and d (different main parameter effects) on higher heating value (HHV).

*3.7.3.2. Ash content.* Fig. 13a, b and c show the $X_1X_2$, $X_1X_3$ and $X_2X_3$ interactions respectively on the Ash, 13d are the main effects of factors on ash content.

The results in Table 6 reveal that only the main and quadratic effect of binder percentage significantly *($p < 0.05$)* influence ash content, with $R^2 = 99.79$ %, justifying the high consistency of the results. The curves in Fig. 13a and b shows that a minimum ash

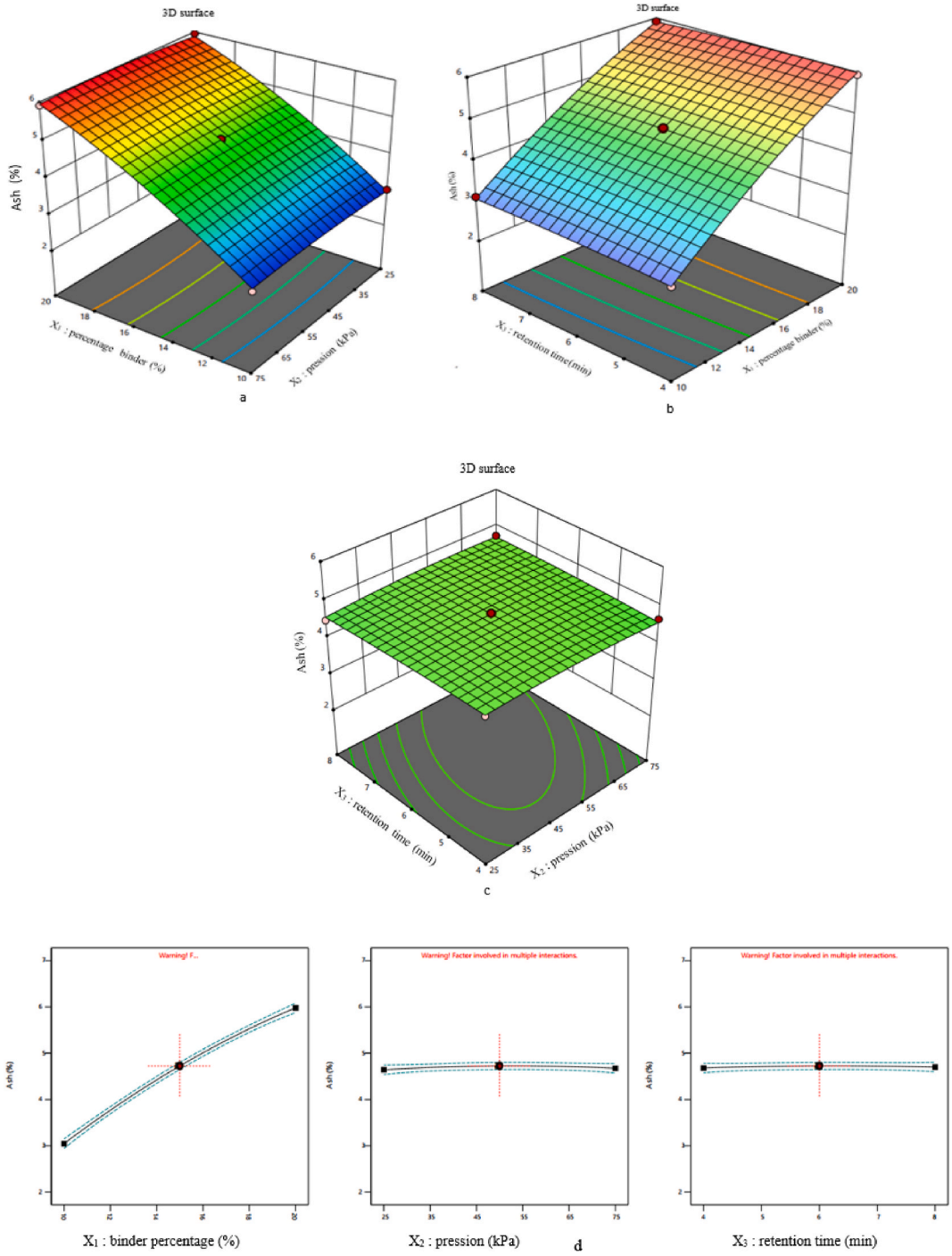


**Fig. 13.** Diagrams of response surfaces (a:$X_1X_2$), (b:$X_1X_3$), (c:$X_2X_3$) and d (main effects of monitored factors) on ash content.

content (approx. 2.9 %) is reached when the percentage of binder is low (10 %). Interestingly, the interactions ($X_1X_2$) and ($X_1X_3$) do not significantly affect ash content ($p > 0.05$). Indeed, despite variations in pressure (25–75 kPa) and time (4–8 min), the ash content remains constant. The same observation is made by (Olugbade et *al.*, 2019). The curve in Fig. 13c shows that the ash content is not affected by variations in parameters $X_2$ and $X_3$. These results concur with observations made by other researchers, notably (Lubwama et *al.*, 2020). The graphs in Fig. 13d clearly illustrate the main effects of the various factors studied on ash content. It is concluded that variations in parameters $X_2$ (compaction pressure) and $X_3$ (retention time) have no significant impact on ash content ($p > 0.05$). On the other hand, ash content is directly related to the increase or decrease in parameter $X_1$ (binder percentage) ($p < 0.05$). A similar

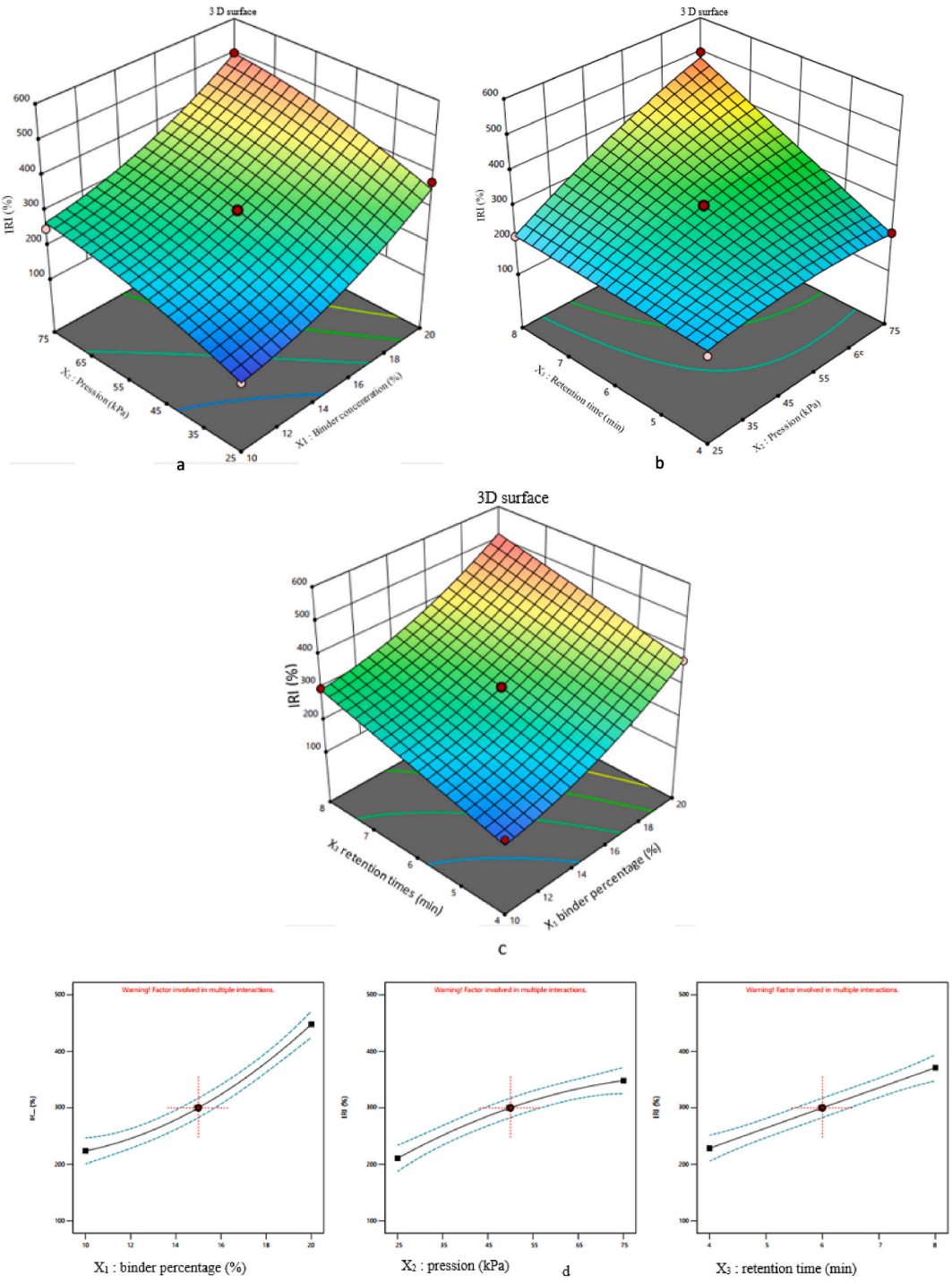


**Fig. 14.** Diagrams of response surfaces for $X_1X_2$ (a), $X_2X_3$ (b) and $X_1X_3$ (c) interactions on the IRI and d, the main effects of parameters on IRI.

observation was made by (Aransiola et *al.*, 2019), reinforcing the validity and reliability of the study's conclusions.

*3.7.3.3. Impact resistance index.* Fig. 14a, b and 14c show the effects of $X_1X_2$, $X_2X_3$ and $X_1X_3$ interactions respectively on IRI and 14d the main effects of parameters on IRI.

According to the results in Table 6, the impact resistance index is significantly influenced ($p < 0.05$) by the three factors and the $X_2X_3$ interaction with $R^2 = 99.10$ %, justifying the strong correlation between these factors and the results. The Analysis of the curves

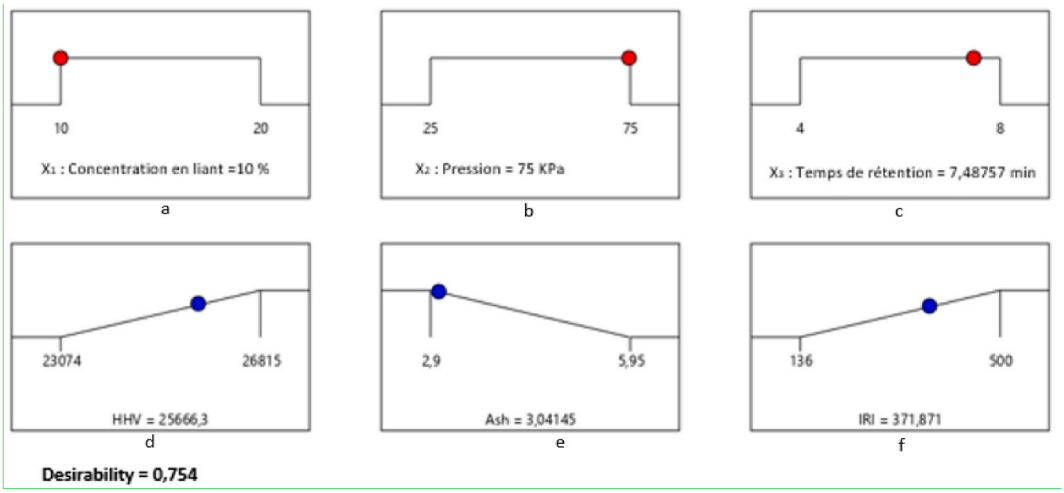


**Fig. 15.** Optimal condition of the composite biofuel production process with carbonized Fraké sawdust: (a, b, c) represent optimal values of binder concentration, compaction pressure and retention time respectively; (d, e, f) are predicted values of HHV, ash content, and IRI respectively.

**Table 6**
ANOVA of the statistical analysis of the different results.

| Sources | Higher heating value (kJ/kg) | Ash content (%) | Impact resistance index (%) |
|---|---|---|---|
| Model | <0.0001[a] | <0.0001[a] | <0.0001[a] |
| $X_1$ | <0.0001[a] | <0.0001[a] | <0.0001[a] |
| $X_2$ | 0.0001[a] | 0.5436 | <0.0001[a] |
| $X_3$ | 0.0002[a] | 0.7062 | <0.0001[a] |
| $X_1X_2$ | 0.0102[a] | 0.5959 | 0.7451 |
| $X_1X_3$ | 0.0012[a] | 0.1881 | 0.8127 |
| $X_2X_3$ | 0.2174 | 0.1881 | <0.0001[a] |
| $X_1^2$ | 0.0433[a] | 0.0005[a] | 0.0027[a] |
| $X_2^2$ | 0.3509 | 0.0979 | 0.0353[a] |
| $X_3^2$ | 0.0184[a] | 0.3583 | 0.9636 |
| $R^2$ | 0.9712 | 0.9979 | 0.9910 |

[a] Factors significant at $p < 0.05$.

in Fig. 15a shows that briquette IRI reaches its peak (500 %) when parameters $X_1$ and $X_2$ are at their maximum levels, i.e., 20 % and 75 kPa respectively. This statement corroborates (Adu-Poku et *al.*, 2022). The Analysis of the curves in Fig. 15b shows that maximum IRI (500 %) is achieved when $X_2$ and X3 are at their highest, i.e., 75 kPa and 8 min respectively. Moreover, the curves in Fig. 15c also show that IRI is at its highest when parameters $X_1$ and $X_3$ are at their highest, i.e., 20 % and 8 min respectively. It is interesting to note that the persuasive effect of retention time on impact resistance index is not consistent with the findings of an earlier study by (Bazargan et *al.*, 2014; Olugbade et *al.*, 2019). This contradiction can be explained by a difference in experimental methods. In their study, they used much higher compaction pressures, ranging from 10 to 100 MPa, for briquette densification, whereas in this study, pressures of 25–75 kPa are used. In summary, it can be stated that when using high compaction pressures, retention time has no significant effect on the IRI of the resulting briquettes. This finding is in line with the results of the study conducted by (Aransiola et *al.*, 2019) who also observed no significant impact of retention time on the impact resistance of briquettes manufactured with high compaction pressures. The graphs in Fig. 14d clearly show the main effects of the various factors on the IRI. The Results confirm that parameters $X_1$, $X_2$ and $X_3$ have a direct influence on IRI. A similar observation was made by (Aransiola et *al.*, 2019) reinforcing the validity and reliability of the study results.

The discrepancies revealed by Figs. 12–14 have prompted further work. For this, it is imperative to determine the optimum operating conditions common to parameters $X_1$, $X_2$ and $X_3$ in order to maximize the properties of the resulting briquettes such as HHV ($Y_1$) and IRI ($Y_3$), but minimize the ash content ($Y_2$). This is to obtain biofuel briquette with high HHV, high IRI and low ash content.

### *3.8. Optimization of the production process of composite biofuels*

To find a compromise between $Y_1$, $Y_2$ and $Y_3$, a desirability function approach is applied using Design Expert version 13. The parameters ($X_1$, $X_2$ and $X_3$) are kept within their specified ranges, while the responses ($Y_1$, $Y_2$ and $Y_3$) are optimized.

The results obtained (Fig. 15) indicate the optimum conditions for the production of quality biofuel briquettes in large quantities from carbonized Fraké sawdust.

The optimum values (Fig. 15) correspond to a binder percentage of 10 % (Fig. 15a), a compaction pressure of 75 kPa (Fig. 15b), and

**Table 7**
Predicted and experimental responses.

| Operating parameters | | | Responses | | | | | |
|---|---|---|---|---|---|---|---|---|
| $X_1$(%) | $X_2$(kPa) | $X_3$(min) | $Y_1$(kJ/kg) | | $Y_2$(%) | | $Y_3$(%) | |
| 10 | 75 | 7,49 | Exp | Pred | Exp | Pred | Exp | Pred |
| | | | 25 596 | 25 666. 3 | 3.01 | 3.04 | 375 | 372 |
| **Standard deviation** | | | **±21.425** | | **±0.021** | | **±2.121** | |

Exp = experimental values; pred = predicted/calculated values.

**Table 8**
Mineralogical composition of the optimized sample.

| Elements | Ni | Pb | Al | Fe | Ca | Zn | Cd | As | Se | Mg |
|---|---|---|---|---|---|---|---|---|---|---|
| Concentration (%) | 0.015 | <LOD | 1.427 | 1.668 | 18.798 | 0.111 | <LOD | <LOD | <LOD | 11.358 |

< LOD: below the Limit of Detection.

a retention time of 7.49 min (Fig. 15c). Predicted results with 75.4 % probability of accuracy are 25 666.30 kJ/kg (Fig. 15d), 3.04 % (Fig. 15e), and 371.88 % (Fig. 15f) for HHV, ash and IRI respectively.

#### *3.8.1. Model validation*

In order to validate the model and the calculation formulas developed, briquettes are produced under previously defined optimum conditions (Fig. 15). Experimental and predicted results are presented in Table 7. The results confirm that the predicted and experimental values match.

### *3.9. Mineralogical analysis with X-ray fluorescence*

After careful analysis of the sample with the X-ray fluorescence spectrometer "Niton XLT900s", the results in Table 8 show the absence of heavy metals such as lead, cadmium, arsenic and selenium, and the very low concentration of zinc and nickel, thus approving the non-dangerousness of the composite biofuels developed.

## 4. Conclusion

This study aimed to model, optimize, and analyze the influence of compaction pressure, binder percentage, and retention time on the higher heating value (HHV), ash content, and impact resistance index (IRI) of briquettes produced from carbonized sawdust. By utilizing the Box-Behnken response surface methodology, researchers determined the optimal parameters for industrial-scale production of biofuels (10 % binder, 75 kPa compaction pressure, and 7.49 min retention time). The results demonstrated that potato peel starch can be successfully used as a binder, replacing cassava starch. Additionally, the study developed mathematical models (equations (15)–(17)) to characterize the briquettes without the need for expensive equipment. Future prospects focus on enhancing the proposed reactor with the aim of recovering synthetic gas.

## Data availability statement

The data associated with this study have not been deposited in a publicly accessible repository!
Data will be made available on request!

## Ethics declarations

✓ Review or approval by an ethics committee was not needed for this study because no data of patients or experimental animals were used.
✓ Informed consent was not required for this study because no clinical data was used.

## Additional information

No additional information is available for this paper.

List of abbreviations and acronyms

| Acronyms | Definitions |
|---|---|
| ANOVA | Analysis of variance |
| AOAC | Association of Official Agricultural Chemists |
| As | Arsenic |
| ASTM-D | American Society for Testing and Materials, |
| Cd | Cadmium |
| F | *Frake* |
| GJ | Giga joule |
| HHV | Higher Heating Value |
| IRI | Impact Resistance Index |
| ISO | International Standards Organization |
| kJ | Kilo joule |
| RSM | Response surface Methodology |
| NF | French standard |

The list of protocols used in this research is as follows:

| Protocol | Parameters studied |
|---|---|
| (NFV 18–100) | Determining the percentage of Protein (%) |
| ASTM D – (3172) | Immediate fuel analysis |
| LUFF Schoorf | Determining of sugar content |
| ISO 10520 | Determining of starch purity |
| ASTM D – (5865) | Determining a fuel's higher heating value |

## CRediT authorship contribution statement

**Nganko Junior Maimou:** Writing – original draft, Software, Methodology, Investigation, Formal analysis, Data curation, Conceptualization. **Koffi Ekoun Paul Magloire:** Writing – original draft, Validation, Supervision, Methodology, Data curation, Conceptualization. **Gbaha Prosper:** Writing – original draft, Validation, Supervision, Methodology, Conceptualization. **Alpha Ousmane Toure:** Validation, Supervision, Methodology, Conceptualization. **Kane Moustapha:** Visualization, Validation, Methodology, Data curation. **Ndiaye Babacar:** Validation, Supervision, Software, Methodology. **Faye Mamadou:** Visualization, Software, Formal analysis. **Nkounga Willy Magloire:** Writing – original draft, Formal analysis. **Tiogue Tekounegning Claudine:** Visualization, Validation, Supervision. **Bile Echua Elisabeth Jasmine:** Writing – original draft, Methodology, Investigation. **Yao Kouassi Benjamin:** Validation, Supervision, Resources, Funding acquisition, Conceptualization.

## Declaration of competing interest

The authors declare that they have no competing financial interests or known personal relationships that would affect the work described in this article.

## Acknowledgements

The authors acknowledge and thank the financial support of the following organizations.

i. French Development Agency (AFD) Through the African Center of Excellence for the Valorization of Waste into High Value-Added Products (CEA-VALOPRO);

ii. The European Union (EU) through the project's Intra-African Academic Mobility Program (RésIng) of the **[624193+RésIng]**.

iii. All anonymous reviewers who agreed to make a significant contribution to the improvement of the manuscript.

## References

[1] P. Caron, J.-M. Châtaigner, A Challenge for the Planet: the Sustainable Development Goals in Debate, Editions Quae, 2017. https://www.torrossa.com/en/resources/an/5064296.

[2] Nations Unies, Sustainable Development Goals, Nations Unies, New York, 2020.

[3] FAO, The State of the World's Forests 2022. Forestry Solutions for Green Recovery and Inclusive, Resilient and Sustainable Economies, FAO, 2022. http://www.fao.org/documents/card/fr/c/cb4834fr.

[4] T. Chungcharoen, N. Srisang, Preparation and characterization of fuel briquettes made from dual agricultural waste : cashew nut shells and areca nuts, J. Clean. Prod. 256 (2020) 120434, https://doi.org/10.1016/j.jclepro.2020.120434.

[5] K. Abo-Amsha, N. Chakraborty, Surface density function and its evolution in homogeneous and inhomogeneous mixture n-heptane MILD combustion, Combust. Sci. Technol. 0 (0) (2023) 1–25, https://doi.org/10.1080/00102202.2023.2182197.

[6] M. Lubwama, V.A. Yiga, Characteristics of briquettes developed from rice and coffee husks for domestic cooking applications in Uganda, Renew. Energy 118 (2018) 43–55, https://doi.org/10.1016/j.renene.2017.11.003.

[7] OECD/FAO, *Agricultural Outlook OECD and FAO 2019-2028* (OECD iLibrary.), Organisation for Economic Co-operation and Development, 2019, https://doi.org/10.1787/agr-outl-data-en.

[8] Weligama Thuppahige, V.T. 2023b.Weligama, L. Moghaddam, Z.G. Welsh, T. Wang, A. Karim, et al., Investigation of critical properties of Cassava (Manihot esculenta) peel and bagasse as starch-rich fibrous agro-industrial wastes for biodegradable food packaging, Food Chem. 422 (2023) 136200. https://doi.org/10.1016/j.foodchem.2023.136200.
[9] B. Théau, R. Kinanga, Guide to Green CharCoal Production, 2021. http://www.initiativesclimat.org/PUBLICATIONS/Guide-production-du-charbon-vert.
[10] AOAC, Official Methods of Analysis, twenty-second ed., AOAC INTERNATIONAL, 2023, 2023, https://www.aoac.org/official-methods-of-analysis/.
[11] N. Boudries, Caractérisation des amidons de sorgho et de mil perlé cultivés dans le Sahara algérien. https://orbi.uliege.be/handle/2268/210187, 2017.
[12] Digestor, 2020.
[13] B.C. Atsé, Potato Production: the Ivorian Association of Agricultural Sciences Relaunches the Project, décembre 12, 2022, https://www.fratmat.info/article/225830/economie/agriculture/production-de-la-pomme-de-terre-lassociation-ivoirienne-des-sciences-agronomiques-relance-le-projet.
[14] D.R. Nhuchhen, Prediction of carbon, hydrogen, and oxygen compositions of raw and torrefied biomass using proximate analysis, Fuel 180 (2016) 348–356, https://doi.org/10.1016/j.fuel.2016.04.058.
[15] International Standard ISO. Physical and mechanical properties of wood—Test methods for small clear wood specimens—Part 2: Determination of density for physical and mechanical tests, 2014. https://www.iso.org/obp/ui/#iso:std:iso:13061:-2:ed-1:v1:en.
[16] S.R. Richards, Physical Testing of Fuel Briquettes, Fuel Process. Technol. 25 (2) (1990) 89–100, https://doi.org/10.1016/0378-3820(90)90098-D.
[17] K.A. Adu-Poku, D. Appiah, K.A. Asosega, N.S.A. Derkyi, F. Uba, E.N. Kumi, E. Akowuah, G.A. Akolgo, D. Gyamfi, Characterization of fuel and mechanical properties of charred agricultural wastes: experimental and statistical studies, Energy Rep. 8 (2022) 4319–4331, https://doi.org/10.1016/j.egyr.2022.03.015.
[18] E.F. Aransiola, T.F. Oyewusi, J.A. Osunbitan, L.A.O. Ogunjimi, Effect of binder type, binder concentration and compacting pressure on some physical properties of carbonized corncob briquette, Energy Rep. 5 (2019) 909–918, https://doi.org/10.1016/j.egyr.2019.07.011.
[19] A. Bazargan, S.L. Rough, G. McKay, Compaction of palm kernel shell biochars for application as solid fuel, Biomass Bioenergy 70 (2014) 489–497, https://doi.org/10.1016/j.biombioe.2014.08.015.
[20] R. Sen, S. Wiwatpanyaporn, A. Annachhatre, Influence of binders on physical properties of fuel briquettes produced from cassava rhizome waste, Int. J. Environ. Waste Manag. 17 (2) (2016) 158–174, https://doi.org/10.1504/IJEWM.2016.076750.
[21] C. Telmo, J. Lousada, Heating values of wood pellets from different species, Biomass Bioenergy 35 (7) (2011) 2634–2639, https://doi.org/10.1016/j.biombioe.2011.02.043.
[22] Production and Forest Industries Department. information present on the survey forms used during data collection from the Direction de la Production et des Industries Forestières of the republic of ivory coast, 2021.
[23] C. Sakkampang, T. Wongwuttanasatian, Study of ratio of energy consumption and gained energy during briquetting process for glycerin-biomass briquette fuel, Fuel 115 (2014) 186–189, https://doi.org/10.1016/j.fuel.2013.07.023.
[24] J. Cai, Y. He, X. Yu, S.W. Banks, Y. Yang, X. Zhang, Y. Yu, R. Liu, A.V. Bridgwater, Review of physicochemical properties and analytical characterization of lignocellulosic biomass, Renew. Sustain. Energy Rev. 76 (2017) 309–322, https://doi.org/10.1016/j.rser.2017.03.072.